Hydrol. Earth Syst. Sci. Discuss., 7, 2347–2371, 2010
www.hydrol-earth-syst-sci-discuss.net/7/2347/2010/

Hydrology and Earth System Sciences Discussions

This discussion paper is/has been under review for the journal Hydrology and Earth System Sciences (HESS). Please refer to the corresponding final paper in HESS if available.

Stream depletion rate with horizontal or slanted wells in confined aquifers near a stream

Pei Rong Tsou[1], **Zheng Yi Feng**[1,*], **Hund Der Yeh**[2], **and Ching Sheng Huang**[2]

[1]Department of Soil and Water Conservation, National Chung Hsing Univ., Taichung, Taiwan
[2]Institute of Environmental Engineering, National Chiao Tung Univ., Hsinchu, Taiwan
[*]now at: National Chung Hsing Univ., Taichung, Taiwan

Received: 22 March 2010 – Accepted: 9 April 2010 – Published: 15 April 2010

Correspondence to: Zheng Yi Feng (tonyfeng@nchu.edu.tw)

Published by Copernicus Publications on behalf of the European Geosciences Union.

Abstract

The stream depletion rate (SDR) associated with pumping from vertical wells located in an aquifer is commonly estimated, where a large drawdown near the well may, however, be produced. In this paper, the solution is first developed for describing the groundwater flow associated with a point source in a confined aquifer near a stream. Based on the principle of superposition, analytical solutions for horizontal and slanted wells are then developed by integrating the point source solution along the well axis. The solutions can be simplified to quasi-steady solutions by neglecting the exponential terms to describe the late-time drawdown, which can provide useful information in designing horizontal well location and length. The direction of the well axis can be determined from the best SDR subject to the drawdown constraint. It is found that hydraulic conductivity in the direction perpendicular to the stream plays a crucial role in influencing the time required for reaching quasi-steady SDR. In addition, the effects of the well length as well as the distance between the well and stream on the SDR are also examined.

1 Introduction

Pumping groundwater near a steam can produce a large amount of water which may partially or totally flow from the stream after a certain period of pumping time. The use of pumping well near a stream is therefore a measure in solving the water deficient problem, especially in an urgent need. A good example is the event happened to the Taoyuan county of Taiwan after the typhoon Matsa occurring on 5 August 2005. The Shihmen reservoir, located at northern part of Taiwan, is the major source of water supply to the Taoyuan county. After the typhoon, the turbidity of the water in Shihmen reservoir reaches 25 000 NTU which exceeds the allowable turbidity of 50 NTU that the water treatment plant can manage. This resulted in more than 630 000 households without having water supply. At that time, the water company drilled wells near the

HESSD

7, 2347–2371, 2010

Taoyuan canal for acquiring the low turbid groundwater which in fact came mostly from the canal. As mentioned in Linsley and Franzini (1979), the groundwater is usually cleared of sediments if flowing through fine-grained materials within a distance of 30 m.

There are many analytical and semi-analytical solutions developed for describing groundwater flow in aquifers with a pumping well located near a stream (e.g., Hunt, 1999; Zlotnik and Huang, 1999; Bulter et al., 2001; Fox et al., 2002; Chen and Yin, 2004; Sun and Zhan, 2007; Bulter et al., 2007; Yeh et al., 2008; Zlotnik and Tartakovsky, 2008). These studies are however based on the problems with a vertical pumping well which may produce a large drawdown cone near the well.

Since 1930s, the horizontal well was used for avoiding some adverse effects involved in the vertical well. In reality, the horizontal well was not widely adopted due to lack of techniques in drilling the wellbore. Recently, the technique of installing the horizontal well has significantly advanced. The problems of obstructions at the ground surfaces such as buildings roads and runways can be avoided now if adopting the horizontal well. In addition, horizontal wells have better contact within the stratum and can be installed in aquifers of small thickness if a long screen length is required. Several previous studies associated with the use of horizontal wells are proposed in the fields of water resources and environmental engineering (e.g., Zhan, 1999; Zhan and Cao, 2000; Park and Zhan, 2002; Park and Zhan, 2003; Zhan and Park, 2003; Kompani-Zare et al., 2005).

Zhan et al. (2001) provided an analytical solution to describe flow toward a horizontal well in an anisotropic confined aquifer. Zhan and Zlotnik (2002) extended point source solution to the cases of slanted wells based on the principle of superposition. Joshi (2003) used horizontal wells to reduce hydrocarbon finding and operating costs. Sun and Zhan (2006) mentioned the use of a horizontal well in an aquitard-aquifer system beneath a water reservoir for water supply. Their results illustrate that the leakage induced from the pumping of the horizontal well is dependent on the well location and length as well as the thickness, storage and vertical hydraulic conductivity of the aquitard.

This paper is first to develop the solutions for describing the behaviors of groundwater flow due to a point source pumping in an anisotropic confined aquifer near a stream. The solutions in terms of head distributions for horizontal and slanted wells are then obtained by integrating the point source solution along the well axis. With the aid of the newly developed solutions, the best orientation and inclination of the well axis can be determined for flow reaching the quasi-steady state. The effects of the aquifer anisotropy, well length, and distance from the well to the stream on the SDR obtained from the horizontal well are also investigated.

2 Methods

2.1 Conceptual model

Figure 1 shows a three-dimensional (3-D) conceptual model for a confined aquifer with a slanted well near a stream. Assume that the aquifer is homogeneous and anisotropic. The origin of coordinate system is located at the interface between the upper boundary of the aquifer and the top of the stream which is considered as the reference datum. The aquifer is of a thickness D and semi-infinite extent in x-direction and infinite extent in y-direction. The length of the well is L and the distance measured from the upper boundary of the aquifer to the middle of the well is z_0 as shown in Fig. 1c. The distance between the stream and the middle of the well is defined as x_0 shown in Fig. 1b. The angles α shown in Fig. 1b and β shown in Fig. 1c represent the orientation and inclination of the well, respectively. Consider two special cases that the slanted well becomes a horizontal well when $\beta = 0$ and is perpendicular to the stream when $\alpha = 0$ shown in Fig. 2a and parallel to the stream when $\alpha = 90^\circ$ shown in Fig. 2b.

The governing equation for describing 3-D transient head distribution $h(x,y,z,t)$ in a confined aquifer with a point source can be expressed as

$$K_x \frac{\partial^2 h}{\partial x^2} + K_y \frac{\partial^2 h}{\partial y^2} + K_z \frac{\partial^2 h}{\partial z^2} = S_s \frac{\partial h}{\partial t} + Q\delta(x - x'_0)\delta(y - y'_0)\delta(z - z'_0), \quad (1)$$

HESSD
7, 2347–2371, 2010

where K_x, K_y, K_z are hydraulic conductivities in the x-, y-, z-directions, respectively; S_s is specific storage; Q is the pumping rate for the point source; $\delta()$ is the Dirac delta function and (x_0', y_0', z_0') is the location of the point source.

The boundary condition along the stream is expressed as

$$h(x = 0, y, z, t) = 0 \tag{2}$$

and the boundary conditions at the top and bottom of the confined aquifer are, respectively,

$$\frac{\partial h}{\partial z}(x, y, z = 0, t) = 0 \tag{3}$$

$$\frac{\partial h}{\partial z}(x, y, z = D, t) = 0. \tag{4}$$

The remote boundary conditions in x- and y-directions are respectively considered as

$$\lim_{x \to \infty} \frac{\partial h}{\partial x} = 0 \tag{5}$$

$$\lim_{y \to \infty} \frac{\partial h}{\partial y} = \lim_{y \to -\infty} \frac{\partial h}{\partial y} = 0. \tag{6}$$

The initial condition is

$$h(x, y, z, t = 0) = 0. \tag{7}$$

The dimensionless variables are introduced as:

$$\begin{aligned} &x_D = \frac{x}{D}, \quad y_D = \frac{y}{D}, \quad z_D = \frac{z}{D}, \\ &x_{0D} = \frac{x_0}{D}, \quad y_{0D} = \frac{y_0}{D}, \quad z_{0D} = \frac{z_0}{D}, \\ &t_D = \frac{K_x}{D^2 S_s} t, \quad L_D = \frac{L}{D}, \quad h_D = \frac{\pi^2 K_x D}{Q} h. \end{aligned} \tag{8}$$

According to Eq. (8), the governing equation can be rewritten as

$$\frac{\partial^2 h_D}{\partial x_D^2} + \kappa_y \frac{\partial^2 h_D}{\partial y_D^2} + \kappa_z \frac{\partial^2 h_D}{\partial z_D^2} = \frac{\partial h_D}{\partial t_D} + \pi^2 \delta(x_D - x_0')\delta(y_D - y_0')\delta(z_D - z_0') \quad (9)$$

where $\kappa_y = K_y/K_x$ and $\kappa_z = K_z/K_x$.

The boundary and initial conditions (2)–(7) become

$$h_D(x_D = 0, y_D, z_D, t_D) = 0 \quad (10)$$

$$\frac{\partial h_D}{\partial z_D}(x_D, y_D, z_D = 0, t_D) = 0 \quad (11)$$

$$\frac{\partial h_D}{\partial z_D}(x_D, y_D, z_D = 1, t_D) = 0 \quad (12)$$

$$\lim_{x_D \to \infty} \frac{\partial h_D}{\partial x_D} = 0 \quad (13)$$

$$\lim_{y_D \to \infty} \frac{\partial h_D}{\partial y_D} = \lim_{y_D \to -\infty} \frac{\partial h_D}{\partial y_D} = 0 \quad (14)$$

$$h_D(x_D, y_D, z_D, t_D = 0) = 0, \quad (15)$$

2.2 Transient head solutions

Applying Fourier transforms to Eqs. (9)–(15) and then inverting the solution in Fourier domain results in

$$h_D(x_D, y_D, z_D, t_D) = 2 \int_0^\infty \int_0^\infty (\Phi_0 + \sum_{n=1}^{\infty} \Phi_n)\, d\xi d\omega \quad (16)$$

with

$$\Phi_0 = \frac{\sin(\omega x_0')\sin(\omega x_D)\cos[(y_0' - y_D)\xi](e^{-(\omega^2+\kappa_y\xi^2)t_D} - 1)}{\omega^2 + \kappa_y\xi^2} \quad (17)$$

and

$$\Phi_n = \frac{2\sin(\omega x_0')\sin(\omega x_D)\cos(n\pi z_0')\cos(n\pi z_D)\cos[(y_0' - y_D)\xi](e^{-(\omega^2+\kappa_y\xi^2+\kappa_z n^2\pi^2)t_D} - 1)}{\omega^2 + \kappa_y\xi^2 + \kappa_z n^2\pi^2} \quad (18)$$

where ω, ξ and n are the variables of Fourier sine, Fourier and finite Fourier cosine transforms, respectively. Note that Eq. (18) contains z_0' which reflects the influence of the depth of the point source on the head distribution in Eq. (16). For detailed derivation of Eq. (16), readers are referred to the Appendix.

Based on the principle of superposition, integrating Eq. (16) along slanted well axis leads to

$$h_{Ds}(x_D, y_D, z_D, t_D) = \frac{1}{L_D}\int_{-\frac{L_D}{2}}^{\frac{L_D}{2}} h_D(x_D, y_D, z_D, t_D)dl \quad (19)$$

with

$$x_0' = l\cos(\alpha)\cos(\beta) + x_{0D}, \quad (20)$$

$$y_0' = l\sin(\alpha)\cos(\beta) \quad (21)$$

and

$$z_0' = l\sin(\beta) + z_{0D} \quad (22)$$

where l is a dummy variable for integration along the slanted well axis.

HESSD
7, 2347–2371, 2010

2.3 Stream depletion rate for pumping in confined aquifers

The SDR herein is defined as the ratio of the quantity of water obtained from the stream to the total amount of water from the well per unit time. The stream is assumed to hydraulically connect with the adjacent aquifer. Therefore, the SDR determined from Darcy's law for the slanted well can be expressed as

$$\frac{q(t_D)_s}{Q} = \frac{1}{\pi^2}\int_{-\infty}^{\infty}\int_0^1 \frac{\partial h_{Ds}}{\partial x_D} dz_D dy_D \quad \text{at} \quad x_D=0 \tag{23}$$

Substituting Eq. (19) into Eq. (23) results in

$$\frac{q(t_D)_s}{Q} = \frac{2}{\pi^2 L_D}\int_{-\infty}^{\infty}\int_{-\frac{L_D}{2}}^{\frac{L_D}{2}}\int_0^{\infty}\int_0^{\infty} \frac{\omega \sin(\omega x_0')\cos[\xi(y_0'-y_D)](e^{-(\omega^2+\kappa_y\xi^2)t_D}-1)}{\omega^2+\kappa_y\xi^2} d\omega d\xi dl dy_D \tag{24}$$

where x_0' and y_0' are defined in Eqs. (20) and (21), respectively. Equation (23) developed based on Eq. (16) implicitly includes the term Φ_n in Eq. (16). The result of integration to z_D for Φ_n in Eq. (23) is zero, indicating that the SDR is independent on the depth of the well.

2.4 Quasi-steady state solution

The quasi-steady solution can be obtained by applying the residue theorem when neglecting the exponential term in Eqs. (17) and (18). The development of quasi-steady state solution form Eq. (16) is shown in Appendix and the result is

$$h_q(x_D, y_D, z_D) = -2\int_0^{\infty}(\frac{1}{2}C_0 + \sum_{n=1}^{\infty} C_n) d\omega \tag{25}$$

where

$$C_0 = -\frac{\sin(\omega x_0')\sin(\omega x_D)e^{-|y_0'-y_D|\sqrt{\frac{\omega^2}{\kappa_y}}}}{\sqrt{\frac{\omega^2}{\kappa_y}}} \tag{26}$$

and

$$C_n = \frac{\sin(\omega x_0')\sin(\omega x_D)\cos(n\pi z_0')\cos(n\pi z_D)e^{-|y_0'-y_D|\sqrt{\frac{\omega^2}{\kappa_y}+\frac{\kappa_z n^2\pi^2}{\kappa_y}}}}{\sqrt{\frac{\omega^2}{\kappa_y}+\frac{\kappa_z n^2\pi^2}{\kappa_y}}}. \tag{27}$$

Based on the principle of superposition, integrating Eq. (25) along the horizontal and vertical well axes yields the hydraulic head distributions in quasi-steady state, respectively, as

$$H_h(x_D, y_D, z_D) = \frac{1}{L_D}\int_{-\frac{L_D}{2}}^{\frac{L_D}{2}} h_q(x_D, y_D, z_D)dy_0' \tag{28}$$

and

$$H_v(x_D, y_D, z_D) = \frac{1}{L_D}\int_{-\frac{L_D}{2}}^{\frac{L_D}{2}} h_q(x_D, y_D, z_D)dz_0'. \tag{29}$$

For the evaluation of Eq. (28), we assume $x_0' = x_{0D}$ in Eq. (26) as well as $x_0' = x_{0D}$ and $z_0' = z_{0D}$ in Eq. (27). Similarly, we assume $x_0' = x_{0D}$ and $y_0' = y_{0D}$ in both Eqs. (26) and (27) for the evaluation of Eq. (29).

3 Results and discussion

3.1 Effects of well length and distance on SDR

Figure 3 shows the SDR from the horizontal well parallel to the stream versus t_D for $\kappa_y = 1$, $\kappa_z = 1$, $L_D = 1$, and various dimensionless distance x_{0D}. The curve of $x_{0D} = 8$ shows that the SDR approaches constants when t_D exceeds 1200, indicating that the present solution reaches quasi-steady state. The figure indicates that the well with a smaller x_{0D} has a higher SDR and reaches the quasi-steady state more quickly. This is because the smaller distance between the stream and well, the less time required for the stream water reaching the well. Therefore, the distance x_{0D} is an important factor in affecting the SDR.

Figure 4 shows the curves of the SDR versus the dimensionless time t_D for the point source as well as the horizontal well parallel and perpendicular to the stream for $\kappa_y = 1$, $\kappa_z = 1$, $x_{0D} = 8$ and $L_D = 10$. The dimensionless well length L_D may range from 2 to 10 when the thickness of the aquifer is 10 m. When $L_D = 10$, the difference in predicted SDR between the point source solution and the solution of the horizontal well parallel to the stream is very small, indicating that the effect of well length on the SDR is negligible. Such a result can be attributed to the fact that the stream is considered as infinitely extended and the horizontal well can therefore be considered to be a point source even if the well length is long. The SDR predicted from the point source solution is smaller than that predicted from the solution of the horizontal well perpendicular to the stream when t_D is in the range of $100 \sim 600$. This is because the horizontal well extends the half well length toward the stream and thus is relatively closer to the stream than the location of the point source. However, the SDR from the solution of the horizontal well perpendicular to the stream is smaller when $t_D > 600$ and reaches quasi-steady state more slowly than that from the point source. This is because the other half of the horizontal well extending toward inland has a longer distance measured from the stream. Therefore, the effect of the well length on the SDR is small.

3.2 Best orientation α and inclination β for less time required for reaching quasi-steady state

Figure 5 shows the contour for the dimensionless time required for reaching quasi-steady state for $\kappa_y = 1$, $\kappa_z = 1$, $x_{0D} = 4$, $L_D = 1$, and various orientation α and inclination β. This figure shows that the smallest time is 1290 for $\alpha = 90^\circ$ or $\beta = 90^\circ$, which indicates the smallest time for the groundwater flow system reaching quasi-steady state occurs in the case of the vertical well or horizontal well parallel to the stream. The dashed lines divide this figure into three regions. The contour lines in the region I for β close to 90° are almost horizontal, indicating that the effect of α on the time of reaching quasi-steady state is negligible. In contrast, the contour lines in the region III for α near 90° are nearly vertical, indicating β has little influence on the time for reaching quasi-steady state. In the region II, both α and β, however, have obvious effect on the time for reaching quasi-steady state. Therefore, the smallest time for reaching quasi-steady state occurs in the case of $\alpha = 90^\circ$ or $\beta = 90^\circ$.

3.3 Effect of anisotropic aquifer on the time required for reaching quasi-steady state

The aquifer near the stream is very likely anisotropic due to the sediment depositional process over a long period of time. The curves of the time for reaching quasi-steady state for $x_{0D} = 4$, $L_D = 1$, and various values of K_x and K_y are shown in Fig. 6. All of the curves are vertical indicating that K_y has no influence on the time for reaching quasi-steady state. Obviously, the K_x is the key factor in influencing the time for reaching quasi-steady state and the SDR reaches quasi-steady state more quickly when K_x is large.

HESSD

7, 2347–2371, 2010

3.4 Drawdown of horizontal and vertical wells

Figure 7 shows the curves of the quasi-steady head distributions versus dimensionless distance x_D for $\kappa_y = 1$, $\kappa_z = 1$, $x_{0D} = 4$, $L_D = 1$, and various dimensionless horizontal well depth z_{0D}. This figure shows that the drawdown produced by the horizontal well is smaller than that by the vertical well of full penetration when z_{0D} is larger than 0.3. In addition, the figure also shows that the drawdown will be smaller if the horizontal well is deeper. On the other hand, Fig. 8 demonstrates the dimensionless head distribution versus x_D for $\kappa_y = 1$, $\kappa_z = 1$, $x_{0D} = 4$, $z_{0D} = 0.2$, and various L_D. The drawdown produced by the horizontal well is significantly smaller than that by the vertical well of full penetration when $L_D > 1.4$, indicating that a larger L_D results in a smaller drawdown. In addition, the horizontal well with a large L_D produces shallow drawdown cones of wide extent as shown in Fig. 8, while the deep horizontal well produces tight drawdown cones as shown in Fig. 7. This indicates that the use of a long well length in producing small drawdown is more effective than that of a deep horizontal well.

4 Concluding remarks

A 3-D point source solution for describing the head distribution of the confined aquifer near a stream is developed by applying Fourier transforms. The aquifer is assumed to be homogenous and the nearby stream is considered as a constant-head boundary. Integrating the point source solution along the well axis yields the analytical solutions for the horizontal and slanted wells. In addition, the quasi-steady solutions can be obtained by neglecting the exponential terms in the solutions. The effects of the horizontal well length and distance between the well and stream on the SDR are investigated. The best direction of well axis can be determined from the smallest time required for reaching the quasi-steady groundwater flow system. In addition, the influences of anisotropy on the time for reaching quasi-steady state are also addressed. The following conclusions can be drawn from this study:

HESSD
7, 2347–2371, 2010

1. The SDR is almost independent on the length of the horizontal well. The SDR reaches quasi-steady state more quickly if the well is closer to the stream.

2. To avoid producing large drawdown and have less time for reaching quasi-steady SDR, the horizontal well would be better to install parallel to the stream.

3. The K_x plays the key role in effecting the time for reaching quasi-steady SDR while K_y has no influence on the time for reaching quasi-steady SDR.

4. The use of a long horizontal well in producing small drawdown is better than that of a deep one under a constant pumping rate.

Appendix A

Mathematical background

Applying finite Fourier cosine, Fourier sine and Fourier transforms to the variables z_D, x_D and y_D in Eqs. (9)–(15), respectively, leads to a first-order ordinary differential equation and initial condition in term of t_D. Solving the ordinary differential equation and then using inverse Fourier transform yield Eq. (16).

The quasi-steady state solution by neglecting the exponential terms in Eqs. (17) and (18) can be expressed in terms of imaginary unit i as

$$h_q(x_D, y_D, z_D) = -2\int_0^\infty \left(\frac{1}{2}\Omega_0 + \sum_{n=1}^{\infty}\Omega_n\right)d\omega \tag{A1}$$

in which

$$\Omega_0 = \mathrm{Re}\left[\int_{-\infty}^{\infty} \frac{\sin(\omega x_0')\sin(\omega x_D)e^{(y_0'-y_D)\xi i}}{\omega^2 + \kappa_y\xi^2} d\xi\right] \tag{A2}$$

HESSD
7, 2347–2371, 2010

and

$$\Omega_n = \mathrm{Re}\left[\int_{-\infty}^{\infty} \frac{\sin(\omega x_0')\sin(\omega x_D)\cos(n\pi z_0')\cos(n\pi z_D)e^{(y_0'-y_D)\xi i}}{\omega^2+\kappa_y\xi^2+\kappa_z n^2\pi^2} d\xi\right]. \quad \text{(A3)}$$

where Re represents the real part of the left-hand side terms in Eqs. (A2) and (A3).

A close path of integration shown in Fig. 9 with a straight line parallel to the real axis and semicircle BCA is constructed for the integrations of Eq. (A3). According to Jordan's Lemma (Folland, 2002), the integration over the semicircular path BCA in Fig. 9a tends to zero when $y_{0D}-y_D>0$ and $R\to\infty$. In contrast, the result of integration over the path BCA in Fig. 9b always tends to zero when $y_{0D}-y_D<0$ and $R\to\infty$.

Based on the residue theorem, the result of integration for Eq. (A3) can be expressed as

$$\Omega_n = 2\pi i \mathrm{Res}\big|_{\xi=p_1} \quad \text{for} \quad y_{0D}-y_D>0 \quad \text{(A4)}$$

and

$$\Omega_n = 2\pi i \mathrm{Res}\big|_{\xi=p_2} \quad \text{for} \quad y_{0D}-y_D<0 \quad \text{(A5)}$$

where p_1 and p_2, singularities, represent $i\sqrt{(\omega^2+\kappa_z n^2\pi^2)/\kappa_y}$ and $-i\sqrt{(\omega^2+\kappa_z n^2\pi^2)/\kappa_y}$ in complex plane, respectively. The residues of the singularities can be estimated by following formulas (Kreyszig, 1999).

$$\mathrm{Res}\big|_{\xi=p_1} = \lim_{\xi=p_1}\Omega_n\cdot(\xi-p_1) \quad \text{for} \quad y_{0D}-y_D>0 \quad \text{(A6)}$$

and

$$\mathrm{Res}\big|_{\xi=p_2} = \lim_{\xi=p_1}\Omega_n\cdot(\xi-p_2) \quad \text{for} \quad y_{0D}-y_D<0 \quad \text{(A7)}$$

Substituting Eqs. (A6) and (A7) into Eqs. (A4) and (A5), respectively and taking the real part of these two results yield

$$\Omega_n = \frac{\sin(\omega x_0')\sin(\omega x_D)\cos(n\pi z_0')\cos(n\pi z_D)e^{-(y_0'-y_D)\sqrt{\frac{\omega^2}{\kappa_y}+\frac{\kappa_z n^2\pi^2}{\kappa_y}}}}{\sqrt{\frac{\omega^2}{\kappa_y}+\frac{\kappa_z n^2\pi^2}{\kappa_y}}} \quad \text{for} \quad y_{0D}-y_D>0 \quad \text{(A8)}$$

and

$$\Omega_n = \frac{\sin(\omega x_0')\sin(\omega x_D)\cos(n\pi z_0')\cos(n\pi z_D)e^{(y_0'-y_D)\sqrt{\frac{\omega^2}{\kappa_y}+\frac{\kappa_z n^2\pi^2}{\kappa_y}}}}{\sqrt{\frac{\omega^2}{\kappa_y}+\frac{\kappa_z n^2\pi^2}{\kappa_y}}} \quad \text{for} \quad y_{0D}-y_D<0 \quad \text{(A9)}$$

The exponential term in Eq. (A9) is equal to that in Eq. (A8) when the term $y_0' - y_D$ in Eq. (A9) is less than zero. Therefore, the integration of Eq. (A3) results in Eq. (27). Otherwise, substituting $n = 0$ into Eq. (27) leads to Eq. (26) which is the result of integration of Eq. (A2).

Acknowledgements. This study was partly supported by the Taiwan National Science Council under the grant NSC 97-2313-B-005-042-MY3.

References

Butler, J. J., Zlotnik, B. A., and Tsou, M.S.: Drawdown and stream depletion produced by pumping in the vicinity of a partially penetrating stream, Ground Water, 39, 651–659, 2001.

Butler, J. J., Zhan, X., and Zlotnik, V. A.: Pumping-Induced Drawdown and Stream Depletion in a Leaky Aquifer System, Ground Water, 45, 178–186, 2007.

Chen, X. and Yin, Y.: Semianalytical solutions for stream depletion in partially penetrating streams, Ground Water, 42, 92–96, 2004.

Folland, G. B.: Advanced calculus, Prentice Hall, New Jersey, 2002.

Fox, G. A., DuChateau, P., and Durnford, D. S.: Analytical Model for aquifer response incorporating distributed stream leakage, Ground Water, 40, 378–384, 2002.
Hunt, B.: Unsteady stream depletion from ground water pumping, Ground Water, 37, 98–102, 1999.
Joshi, S. D.: Cost/Benefits of horizontal wells, Society of Petroleum Engineers, 19–24, 2003.
Kompani-Zare, M., Zhan, H., and Samani, N.: Analytical study of capture zone of a horizontal well in a confined aquifer, J. Hydrol., 307, 48–59, 2005.
Kreyszig, E.: Advanced engineering mathematics, John Wiley & Sons Inc., New York, 1999.
Linsley, R. K. and Franzini, J. B.: Water resources engineering, McGraw-Hill Book Company, New York, 1979.
Park, E. and Zhan, H.,: Hydraulics of a finite-diameter horizontal well with wellbore storage and skin effect in leady aquifers, Adv. Water Resour., 25, 389–400, 2002.
Park, E. and Zhan, H.: Hydraulics of horizontal well in fractured shallow aquifer systems, J. Hydrol., 281, 147–158, 2003.
Sun, D. and Zhan, H.: Flow to a horizontal well in an aquitard-aquifer system, J. Hydrol., 321, 364-376, 2006.
Sun, D. and Zhan, H.: Pumping induced depletion from two streams, Adv. Water Resour., 30, 1016–1026, 2007.
Yeh, H. D., Chang, Y. C., and Zlotnik, V. A.: Stream depletion rate and volume of flow in wedge-shape aquifers, J. Hydrol., 349, 501–511, 2008.
Zhan, H.: Analytical study of capture time to a horizontal well, J. Hydrol., 217, 46–54, 1999.
Zlotnik, V. A. and Huang, H.: Effect of shallow penetration and streambed sediments on aquifer response to stream stage fluctuations (analytical model), Ground Water, 37, 599–605, 1999.
Zhan, H. and Cao, J.: Analytical and semi-analytical solutions of horizontal well capture times under no-flow and constant-head boundaries, Adv. Water Resour., 23, 835–848, 2000.
Zhan, H., Wang, L. V., and Park, E.:On the horizontal-well pumping tests in anisotropic confined aquifers, J. Hydrol., 252, 37–50, 2001.
Zhan, H. and Zlotnik, V. A.: Ground water flow to horizontal and slanted wells in unconfined aquifers, Water Resour. Res., 38, 1108, doi:10.1029/2001WR000401, 2002.
Zhan, H. and Park, E.: Hydraulics of horizontal wells in leaky aquifers, J. Hydrol., 281, 129–146, 2003.
Zlotnik, V. A. and Tartakovsky, D. M.: Stream depletion by groundwater pumping in leaky aquifers, J. Hydrol. Eng., 13, 43–50, 2008.

HESSD
7, 2347–2371, 2010

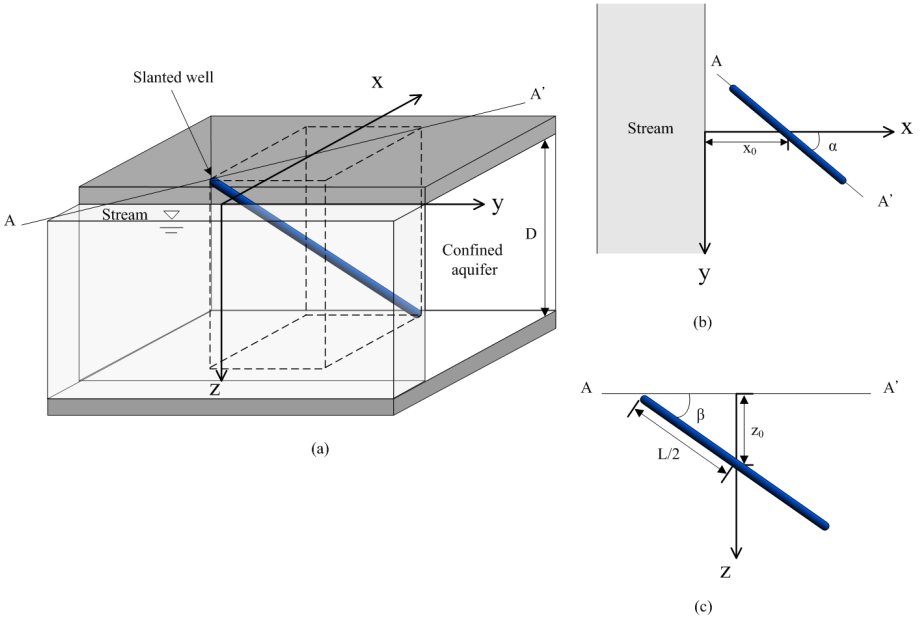

Fig. 1. Schematic diagram. **(a)** 3-D view **(b)** top view **(c)** view of vertical plane including cross section A–A'.

HESSD
7, 2347–2371, 2010

Stream depletion rate with horizontal or slanted wells

Pei Rong Tsou et al.

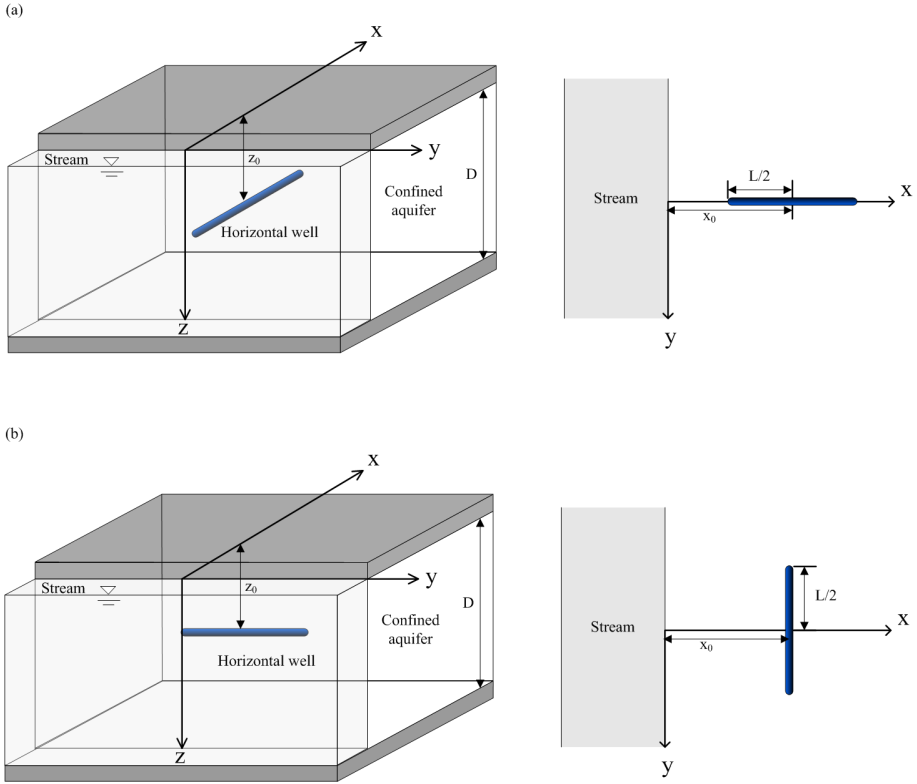

Fig. 2. Schematic diagram of horizontal well for $\beta = 0$ and $\alpha =$ **(a)** 0 **(b)** 90°.

HESSD
7, 2347–2371, 2010

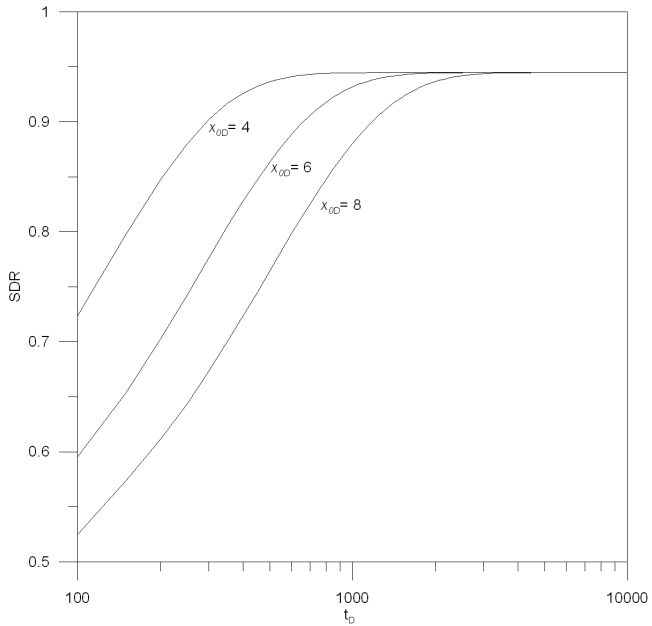

Fig. 3. The SDR from the horizontal well parallel to the stream versus dimensionless time for $\kappa_y = 1$, $\kappa_z = 1$, $L_D = 1$, and various distance between the well and stream.

HESSD
7, 2347–2371, 2010

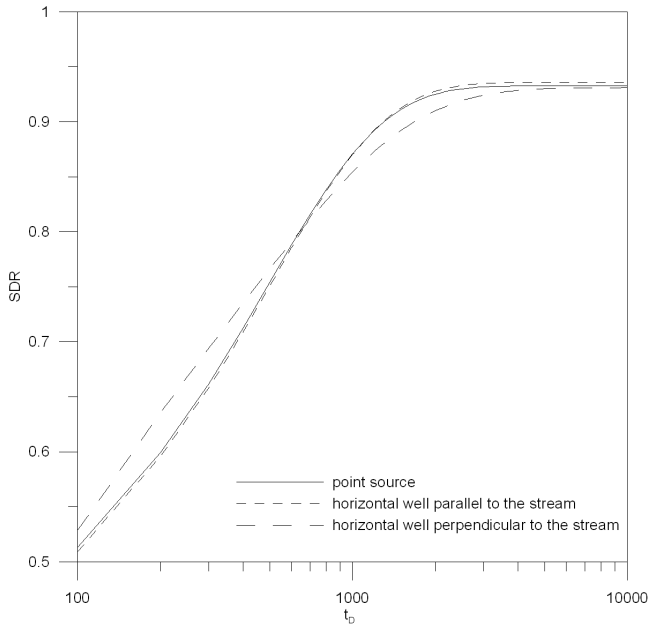

Fig. 4. Comparison of the SDR obtained from the point source and the horizontal well parallel and perpendicular to the stream for $\kappa_y = 1$, $\kappa_z = 1$, $x_{0D} = 8$ and $L_D = 10$.

HESSD

7, 2347–2371, 2010

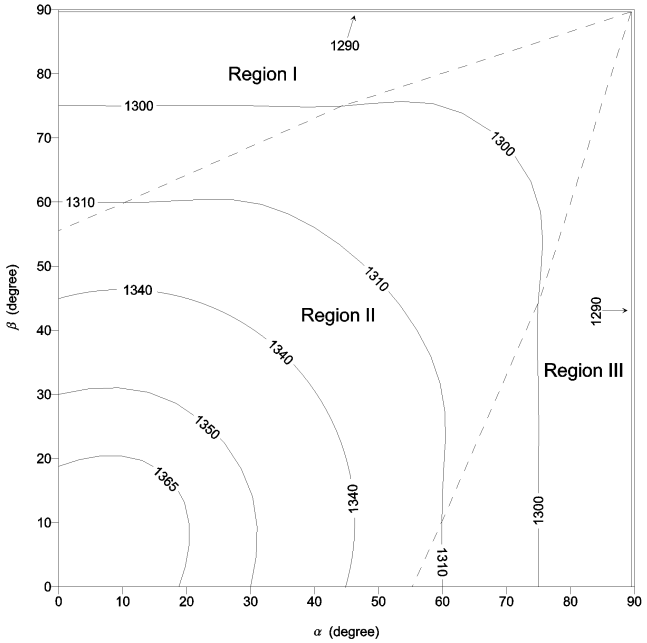

Fig. 5. Contours for the time for reaching quasi-steady state SDR for $\kappa_y = 1$, $\kappa_z = 1$, $x_{0D} = 4$, $L_D = 1$, and various orientation α and inclination β.

HESSD
7, 2347–2371, 2010

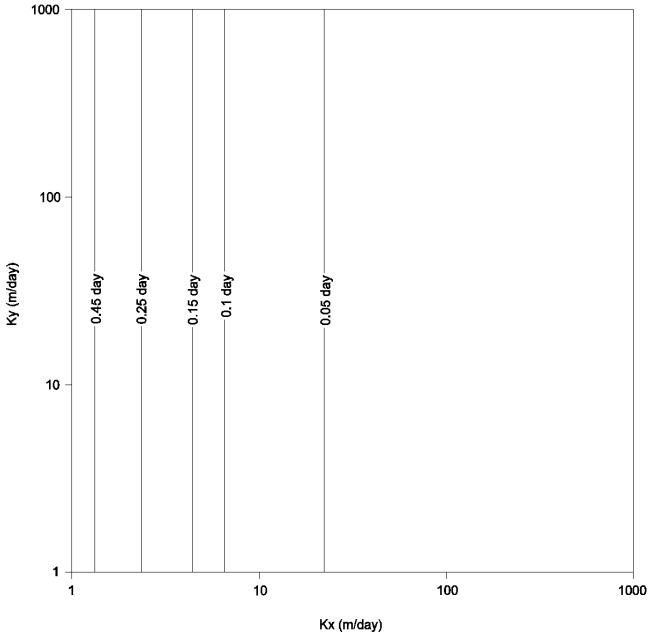

Fig. 6. Contours for the time for reaching quasi-steady state SDR for $x_{0D} = 4$, $L_D = 1$, and various hydraulic conductivities K_x and K_y.

HESSD

7, 2347–2371, 2010

Stream depletion rate with horizontal or slanted wells

Pei Rong Tsou et al.

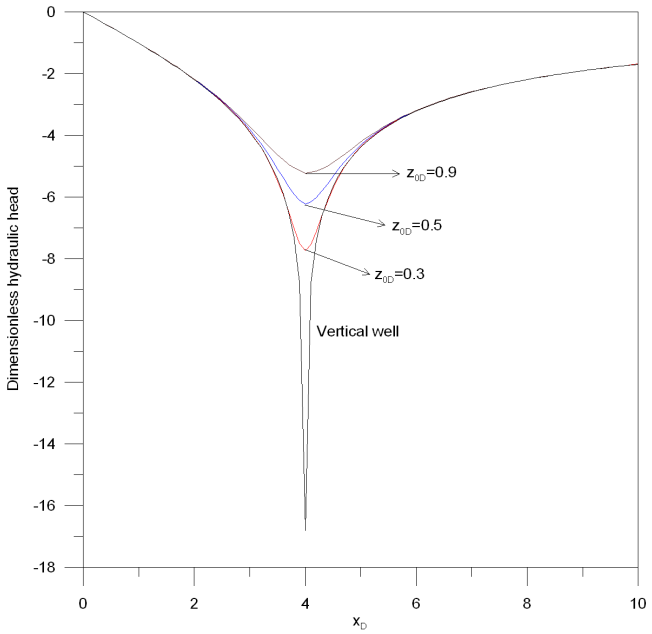

Fig. 7. The spatial head distribution for $\kappa_y = 1$, $\kappa_z = 1$, $x_{0D} = 4$, $L_D = 1$, and various depth of the horizontal well parallel to the stream.

HESSD

7, 2347–2371, 2010

Stream depletion rate with horizontal or slanted wells

Pei Rong Tsou et al.

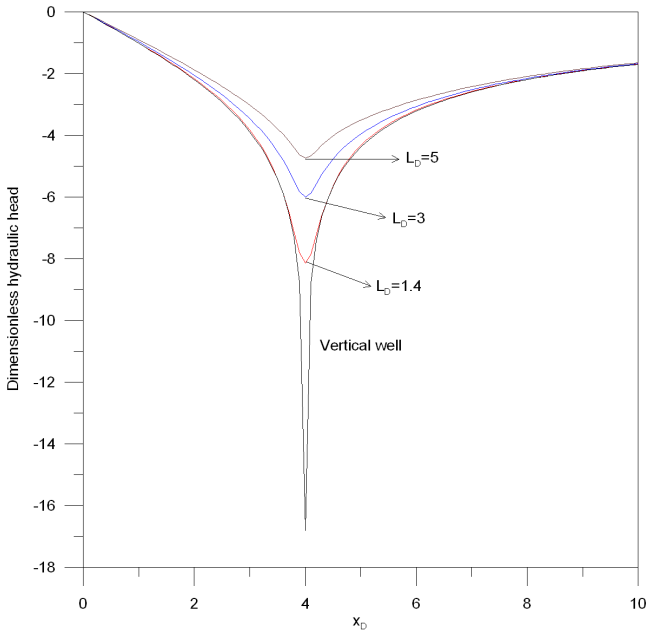

Fig. 8. The spatial head distribution for $\kappa_y = 1$, $\kappa_z = 1$, $x_{0D} = 4$, $z_{0D} = 0.2$, and various length of the horizontal well parallel to the stream.

HESSD
7, 2347–2371, 2010

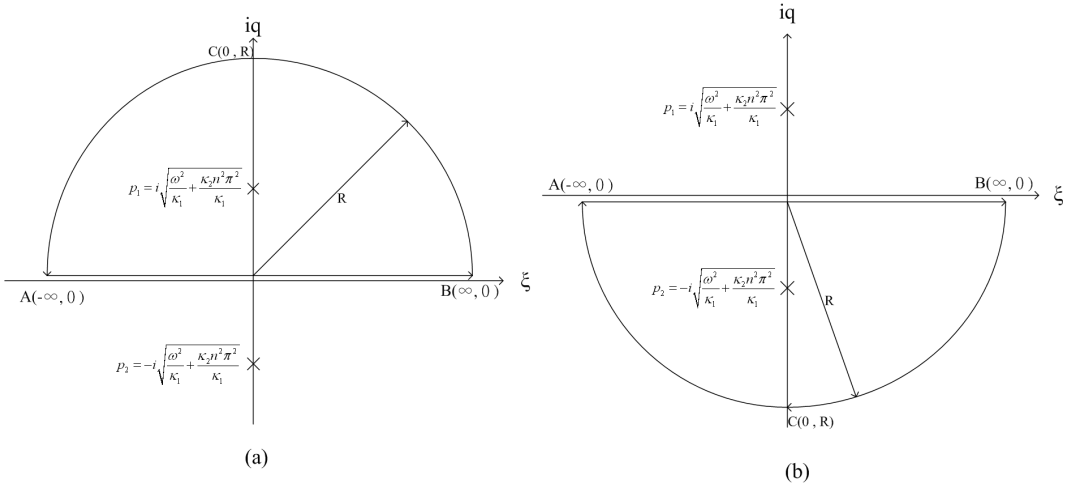

Fig. 9. Contour of integration.

HESSD
7, 2347–2371, 2010